Effect of growth conditions on the physical properties of the sulfosalt $SnSb_2S_4$ thin films deposited by the thermal vacuum evaporation technique

A. GASSOUMI*, M.KANZARI
Laboratoire de Photovoltaïque et Matériaux Semi-conducteurs – ENIT- Tunis El Manar University, BP 37, Le belvédère 1002-Tunis, Tunisie

The initial ingot of the $SnSb_2S_4$ material was prepared by the horizontal Bridgman method. X-rays diffraction analysis of the powder showed that only homogenous $SnSb_2S_4$ phase is present in the ingot. $SnSb_2S_4$ thin films were deposited on heated glass substrates by a thermal vacuum evaporation of the crushed powder from the ingot. The substrate temperatures (Ts) were varied in the range 80-240 °C with a step of 40 °C. Here, we investigate the effect of both substrate temperature (Ts) and annealing process on the structural, optical and electrical properties of these films. As the substrate temperature increases and, after annealing under air atmosphere, the average grain size increases from 240 to 420 Å. The switching phenomena are also discussed on the basis of thermally induced transformations.

(Received January 19, 2012; accepted April 11, 2012)

Keywords: $SnSb_2S_4$ thin films, structural properties, morphological properties, optical properties, electrical properties.

1. Introduction

In recent years, more attention has been given to the sulfosalt layers owing to their potential applications in many technological applications particularly: thin film solar cells [1-3], thermoelectric energy conversion [4], and various types of sensors [5-8]. The sulfosalt compounds appear to be also potential candidates to expand number of future applications for switching phenomena.

Sulfosalts belong to a class of complex sulfides with the general formula of $A_mB_nX_p$, where A stands for metallic elements like tin Sn and lead Pb; B represents formally trivalent, semi-metallic elements such as arsenic As, antimony Sb, and bismuth Bi; and X can be either sulfur S or selenium Se [9]. $SnSb_2S_4$ is an important semiconducting material and has been partially investigated in our previous studies [10-12]. However, the effect of substrate temperature has not yet been studied in details. In the present study, we explore the structural, electrical and optical changes on the $SnSb_2S_2$ thin films in terms of both the annealing under air and the substrate temperature variations. To date, the dependence on the physical properties of such thin films as a function of the substrate temperature has not been yet carried out.

2. Experimental procedure

2.1. Preparation of the $SnSb_2S_4$ ingot

The initial ingot of the $SnSb_2S_4$ material was grown using the horizontal Bridgman method. Stoichiometric amounts of 99.999% pure Sn, Sb, and S were used. The mixture was sealed under vacuum in a quartz tube and heated slowly (10 °C/h). A complete homogenization of the mixture is achieved by keeping the melt at 600 °C for about 48 h. To avoid cracking due to the thermal expansion of the melt upon solidification the tube was cooled at a rate of 10 °C/h. X-ray analysis of the powdered material confirmed that only a homogenous $SnSb_2S_4$ phase was present in the ingot [13]. Then, a crushed powder of this ingot was used as raw material for the thin film deposition by the thermal vacuum evaporation technique.

2.2. Film preparation

Before film deposition, the glass substrate was cleaned using a detergent solution, acetone, and rinsed with de-ionized water, then dried in clean air. The films were deposited onto glass substrates by thermal vacuum evaporation. The pressure during the evaporation was maintained at 10^{-5} Torr. The substrate temperatures (Ts) were varied in 80-240 °C domain with a step of 40 °C and a chromel-alumel thermocouple was used to monitor the Ts variations. The deposited films were therefore annealed for 1h in air at the temperature 275°C.

2.3. Characterization of the evaporated films

The structural properties of the evaporated thin films were determined by X-ray diffraction (XRD) using cobalt $CoK_{\alpha 1}$ radiation (λ=0.1789 nm); the diffraction is carried out in Bragg Brentano symmetric geometry. Optical transmittance and reflectance were measured at normal incidence with a UV–visible–NIR Shimadzu 3100S spectrophotometer in the wavelength range 300–1800 nm.

The surface morphology and roughness of the films were examined by atomic force microscopy (AFM) type Veeco model D3100. The film thicknesses were found to be around 700 nm by using a profilometer type Mitutoyo Surftest-301. The films were thermoelectrically characterized using resistance measurements as function of the air annealing temperature. Finally, the hot probe method measurements were carried out in order to determine the conductivity type of the films.

3. Results and discussion

3.1. Structural and morphological properties

In order to study the dependence of structural properties on the substrate temperature, we investigated the changes in the structural characteristics such as the crystal structure and surface morphology have been investigated by means of XRD and AFM techniques. The analysis of the XRD patterns represented in figure 1, revealed a strong dependence of structural characteristics of the films in terms of the substrate temperature. Careful analysis of the X-ray diffraction pattern of the annealed samples indicates the polycrystalline nature of these thin films. The crystallites are preferentially oriented along (501) planes parallel to the substrate. The intensity of the peak corresponding to (501) plane increases when the substrate temperature increases. It is important to note that no oxide phases were found after annealing in air. In addition, the intensity ratio (I_{501}/I_{621}) increases with increasing the substrate temperature after the annealing process which indicates the prominence of (5 0 1) orientation. On the other hand, to investigate the effect of the annealing process on the crystal grain size we used the relation ship between crystal grain size and X-ray line broadening, as described by Scherrer's equation:

$$D = \frac{0.9\lambda}{\beta \cos\theta} \qquad (1)$$

where D is the average crystallite dimension, λ is the wavelength in angstroms, β is the full-width, half-maximum (FWHM), and θ is Bragg angle, for more detail see ref.[14]. The average crystalgrain sizes of these thin films were evaluated to be in the range of 240 to 420 Å using the 501 diffraction line of the $SnSb_2S_4$ evaporated thin films. The variations of the crystal grain size D versus the substrate temperature for the most prominent (501) peak of $SnSb_2S_4$ is shown in fig. 2. It is noted that the grain size increases with increasing the substrate temperature (Ts).

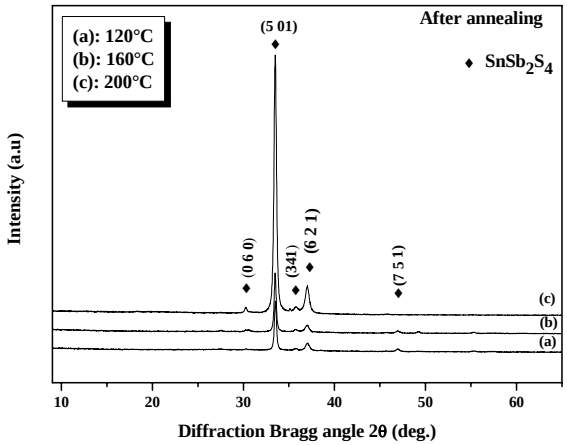

Fig.1. X-ray diffraction patterns of annealed $SnSb_2S_4$ thin films at various substrate temperature.

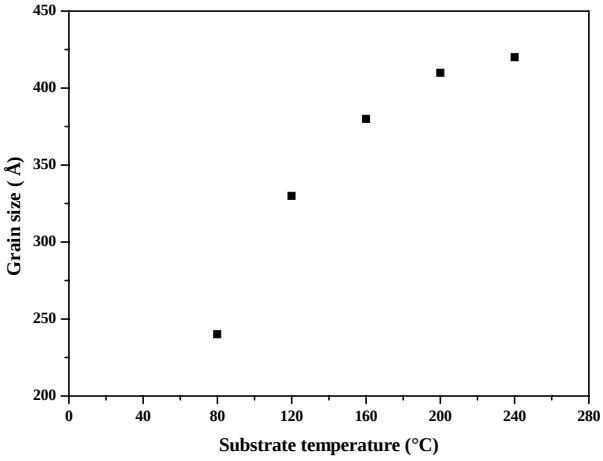

Fig.2. Variation of the grain size with thin films at various substrate temperature.

AFM topographical images of the surfaces are shown in Fig. 3. It can be seen that the films deposited at various substrate temperatures show perturbed surface state. The surface roughness of all these films shows indeed an increase with the substrate temperature. Before the annealing treatment step $SnSb_2S_4$ films have a very smooth surface with a RMS surface roughness ranging from 3.730 to 10.431 nm, whereas after annealing have value increased from 4.127 to 14.199 nm. This can be explained by the fact that film deposited at higher substrate temperature has good crystallinity state. As seen in Fig. 3, the surface morphology of the $SnSb_2S_4$ thin films deposited at low substrate temperatures shows a rude surface with small grains, but after 160°C, the grains become larger and dense and smooth surface is observed.

Upon the increase of the substrate temperature the particles have enough energy to diffuse which results in the formation of a more compact film. This morphological enhancement via 3D AFM observations is consistent with XRD results described above.

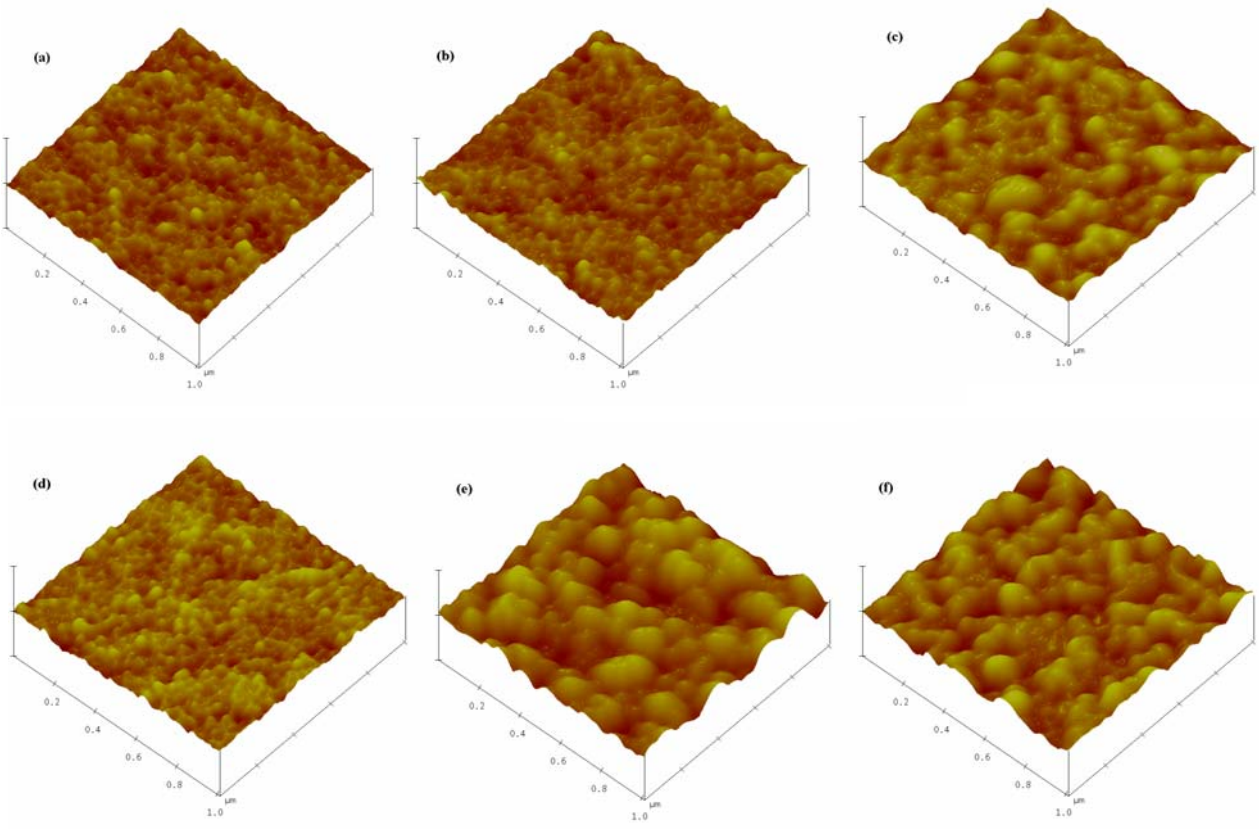

Fig.3. 3D AFM images of $SnSb_2S_4$ films surface: As-grown: (a) 120°C, (b) 160°C, (c) 200°C, Air-annealed films: (d) 120°C, (e) 160°C, (f) 200°C.

3.2. Optical properties

Figs. 4 (a) and (b) show the spectral dependence both of the transmittance (T) and the reflectance (R) at normal incidence, respectively. The transmittance (T) is strongly affected by the thermal treatment of the thin films. In all cases, the films show a decrease in the transmittance and a small increase in the reflectance (R). After annealing the films, the transmittance decreases with the substrate temperature while the reflectance increases with increasing the annealing temperature. It is well known that, the heat treatment leads to an increase of the crystallite size and an improvement of the film crystallinity [15]. It is also know that, the increase in surface roughness of the heat-treated thin films plays a major role in the drastic decrease of optical transmittance [15].

On the other hand, the absorption coefficient α see ref [16] is related to the energy gap E_g according to the following equation [17]:

$$\alpha h\nu = A\left(h\nu - E_g\right)^n \qquad (2)$$

where A is a constant, h is the Planck constant and n is equal to ½ for a direct gap and 2 for an indirect gap semiconductor. The band gap E_g was determined by extrapolating the straight section of the $(\alpha h\upsilon)^2$ vs. *h*ν curve to the horizontal photon energy axis. The band gap is about 1 eV for thin film grown at 120°C. For the films with higher Ts, it is difficult to obtain the energy gap E_g value because the transmittance coefficient of the film is so low.

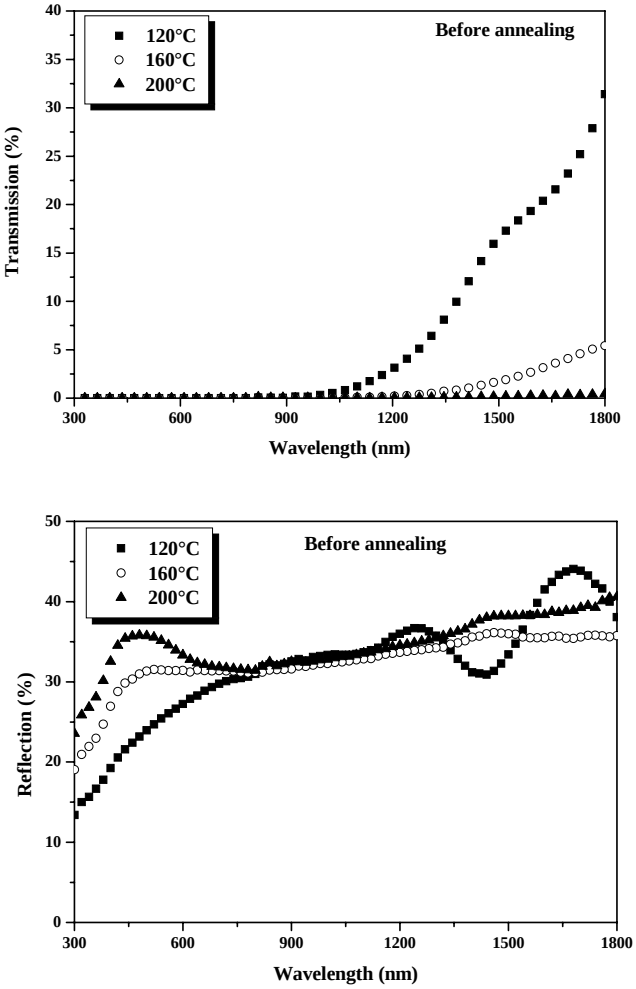

Fig.4. Transmittance (a) and Reflectance (b) spectra of as-deposited $SnSb_2S_4$ thin films at different substrate temperature.

3.3. The electrical properties

The electrical resistance R of the prepared $SnSb_2S_4$ thin films was measured over the annealing temperature and at various substrate temperatures. The electrical contacts were made by applying under the film and at the edges of the substrate two bands of gold separated by about 10 mm.

As shown in Fig. 5, the $SnSb_2S_4$ thin films exhibit a remarkable change in their electrical properties at transition temperatures of about 160 °C, where ρ_i is the resistivity value at 50 °C (heating cycle) and ρ_f the resistivity value at 50 °C (cooling cycle).

From a critical resistivity value, the resistivity drops drastically and the material is converted from a highly resistivity (OFF) into a lowest resistivity (ON) state. In these conditions, the fundamental question is whether the switching is of a thermal or purely electronic nature. During the heating cycle, the electrical resistivity of the film decreases notably with the temperature within the lower temperature range. During the cooling cycle, it is observed that the resistivity increases with temperature following a different cycle than the heating one. After the annealing treatment all films showed p-type conductivity.

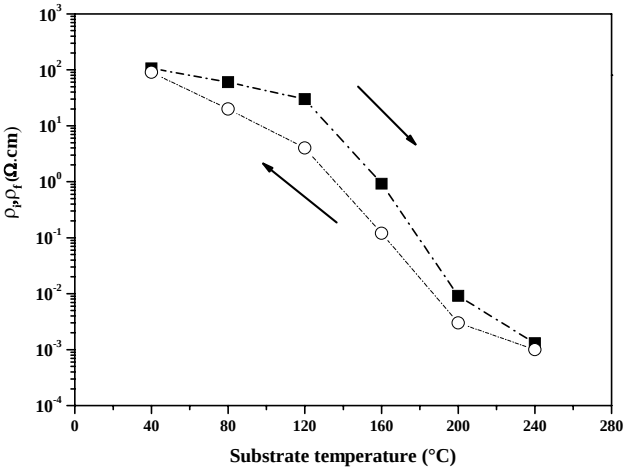

Fig. 5. Variation of the resistivity versus the substrate temperature.

4. Conclusion

Here it is discussed the effects of both the substrate temperature (Ts) and annealing under free air on the structural, optical and electrical properties of $SnSb_2S_4$ thin films grown using thermal vacuum evaporation technique. The structural properties showed an evidence for the presence of only $SnSb_2S_4$ phase and no oxide phases were detected. The grain size and the surface roughness are increases as function of the substrate temperature. On the other hand, we reported a novel electrical switch based on $SnSb_2S_4$ thin films. All the films exhibit stable p-type conductivity after the air annealing. This first result regarding the electrical properties of $SnSb_2S_4$ evaporated thin films seem to be very encouraging since a simple fabrication method has been used. Further, studies on the properties are in progress to understand this commutation effect of such films. Finally, these results demonstrate that the $SnSb_2S_4$ film could be used as a potential candidate in many technological applications such as phase change memory devices.

References

[1] A. Gassoumi, M. Kanzari , J. Optoelectron. Adv. Mater, **11**(4), 414 (2009).
[2] H. Dittrich, K. Herz, J. Eberhard, and G. Schumm, Proc.14th EU Photov. Sol. En. Conf., Barcelona, Spain, 2054 (1997).
[3] M. Y. Versavel, J. A. Haber , Thin Solid Films **515**, 5767 (2007) .
[4] K. Hoang, S.D. Mahanti, J. Androulakis, M. G. Kanatzidis, Mater. Res.Soc. Symp. Proc **886** ,0886-F05–06.1 (2006).

[5] O. L. Kheifets, L. Y. Kobelev, N. V. Melnikova, L. L.Nugaeva, Solid-State Electron, **52**, 86 (2007)**.**
[6] T. Wagner, M. Krbal, P. Nemec, M. Frumar, Th. Wagner,M. Vlcek, V. Perina, A. Mackova, V. Hnatovitz, S. O.Kasap, Appl. Phys. A, **79**, 1563 **(**2004).
[7] J. Gutwirth, T. Wagner, P. Nemec, S. O. Kasap, M. Frumar , J. Non-Cryst. Solids, **354**, 497 (2008).
[8] T. Ohta, J. Optoelectron. Adv. Mater, **3**(3), 609 (2001).
[9] G. N. Kryukova, M. Heuer, G. Wagner, T. Doering, K. Bente, Journal of Solid State Chemistry **178**, 376 (2005).
[10] A. Gassoumi, M. Kanzari , J. Optoelectron. Adv. Mater. **12**(5), 1052 (2010).
[11] A. Gassoumi, M. Kanzari , Physica E: Low-dimensional Systems and Nanostructures **44**, 71 (2011).
[12] A. Gassoumi, M. Kanzari , B. Rezig , EPJ Applied Physics, **41**(2), 91 (2008).
[13] P. Smith, J. Parise , Acta Cryst. B, **41**, 84 (1985)**.**
[14] S. F. Bartram ,Handbook of X-Rays, edited by E.F. Kaelebe ,McGraw-Hill, New York. Chapter 17 (1967) .
[15] N. Ţigau, C. Gheorghieş, G.I. Rusu S. Condurache-Bota, Journal of Non-Crystalline Solids **351**, 987 (2005).
[16] T.S. Moss, Optical Properties of Semiconductors (Butterworth, London) (1959).
[17] E. A. Davis, N. F. Mott , Philipp. Mag, **22**, 903 (1970).

*Corresponding author: abdelaziz.gassoumi@gmail.com